ROLE OF SnO_2 NANOPARTICLE ADDITIONS AND ANNEALING TREATMENT ON THE CRYSTAL STRUCTURE AND OPTICAL PROPERTIES OF TiO_2 THIN FILM

M.M.A. Alhaffar[1], F.K. Dahash[2], S.N.S. Al-Humairi[3*], M.H. Almaamori[4]

[1]College of Materials Engineering, University of Babylon, 51001 Hillah, Babil, Iraq.

[2]Department of Radiology and Sonar, College of Medical Technology, The Islamic University, Najaf, Iraq.

[3]Faculty of Information Sciences and Engineering, Management and Science University, 40100 Shah Alam, Malaysia.

[4]Prosthetics & Orthotics Engineering Department, College of Engineering, AL-Mustaqbal University, 51001 Hillah, Babil, Iraq

*Corresponding Author's Email: safaa_najah@msu.edu.my

Article History: Received 8 October 2024; Revised 18 June 2026; Accepted 16 July 2026

ABSTRACT: This study investigates the effect of varying SnO_2 percentages on the structural properties of TiO_2 thin films. The bare and doped samples were prepared using the spray pyrolysis technique (SPT) by deploying TiO_2 as a precursor. The crystal structural parameters were investigated using X-ray diffraction (XRD), and it was found that the bare sample exhibited a permanent anatase phase of TiO_2. However, this phase transformed into the rutile phase upon doping with 9% SnO_2. Furthermore, the rutile phase intensity decreased when the prepared thin film was annealed at 250°C for 90 minutes. UV-vis spectroscopy was used to investigate the effect of SnO_2 doping on the optical properties of TiO_2. The results revealed that doping with SnO_2 significantly decreased the transmittance of the TiO_2 thin film. On the other hand, the absorbance value of the TiO_2 thin film increased to the highest

value with the doping of 9 at.% of SnO_2. In conclusion, the results of structural changes and optical properties depicted the effectiveness of SnO_2.

KEYWORDS: *Thermal chemical spraying technique, TiO_2 membranes, structural properties.*

1.0 INTRODUCTION

Recent advancements in various applications, such as light-emitting diodes, supercapacitors, gas sensors, anti-reflective coatings, optical waveguides, optoelectronics, photonic crystals, and semiconductor-based devices, have highlighted the potential of transition conducting oxide (TCO) thin films [1, 2]. Among these oxides, titanium dioxide (TiO_2) stands out due to its exceptional physical and chemical properties, including high transmittance (~80%), wide bandgap, high refractive index, and excellent thermal and chemical stability [3, 4]. These are the three phases of crystallization for TiO_2: rutile, tetragonal anatase, and orthorhombic brookite [5, 6]. Among these three, the anatase phase is most commonly used due to its effective mass, reasonable cost, and stability against hydrogen plasma atmospheres in the production of solar cells [7]. Therefore, several research studies have focused on utilizing the solar spectrum by TiO_2 to optimize its microstructural and optical properties for various environmental applications. The anatase modification of TiO2 is an outstanding material due to its unique chemical, optical, electrical, and electronic properties [8]. The ability to absorb UV radiation enhances the chemical stability and mechanical strength of this material. These features enable TiO2 to serve a wide range of applications across various areas.

Most importantly, TiO2 has high photocatalytic activity in the anatase phase, which helps reduce environmental pollution through photocatalysis [9, 10]. Thin TiO_2 films are also used as photoelectrodes in waveguiding applications and for gas sensing. The TiO_2 layers exhibit excellent surface reactions that either facilitate the reduction or oxidation of gases, thereby influencing the conduction properties of the membranes [11]. Various techniques have been employed to deposit thin films with desired characteristics [12], such as magnetron sputtering [13], pulsed laser deposition [14, 15], spray pyrolysis [16, 17], sol-gel methods [18], and the chemical bath deposition (CBD) technique [19, 20]. The Spray Pyrolysis technique (SPT) method primarily involves the chemical decomposition of compounds to form

stable material precipitates [21]. In this process, thin films are deposited on heated substrates through a gaseous flow that atomizes the solution via capillary tubes of the spraying device [22]. The reactants are chemical entities in which the unwanted material vaporizes at the temperature corresponding to sedimentation. SPT is particularly suitable for creating thin films from ceramic materials, powders, and their oxides, offering benefits such as simplicity, cost-effectiveness, ease of adding materials in varying proportions, high growth rates, and the capability to produce uniform coatings over large areas [23]. Introducing suitable impurities to modulate the doping of wide-band-gap TiO2 can significantly alter its electrical, optical, and structural properties. Prior research has documented the impact of transition metals, such as Zn, Mn, Fe, Ni, Er, and Co, on TiO2 thin films, with a focus on controlling these various properties. Patil et al. [24] deposited Ni-doped, spray-pyrolyzed nanostructured TiO_2 thin films and found that the presence of Ni significantly influenced the surface properties of these films.

On the other hand, Zn was also chosen as the dopant element for the parent sample. The selection of Zn is based on several factors: the ionic radius of Zn (0.60 Å) closely matches that of Ti (0.68 Å) [25], which suggests that Zn^{2+} can integrate into the TiO_2 lattice or occupy interstitial sites without compromising the crystal structure, thus stabilizing the anatase phase [26]. Arunachalam et al. [27] observed that the presence of the transition metal zinc notably influenced the crystallite size of titanium dioxide (TiO_2), reducing from 17.092 nm to 4.955 nm. The band gap energy reduction, from 3.45 eV to 3.38 eV, was reported by Naffouti et al. [23], who doped TiO2 thin films previously deposited by the SPD technique with manganese. Despite these advances, a comprehensive understanding of the specific structural and optical effects induced by tin oxide (SnO2) doping in TiO2 thin films remains elusive. While the potential benefits of doping are recognized, the intricate interplay between SnO_2 concentration and subsequent thermal annealing treatments on the crystallographic phase evolution (particularly the critical anatase-to-rutile transformation) and the resultant optical response (transmittance and absorbance across relevant spectral ranges) warrants further systematic investigation. Elucidating these relationships is crucial for achieving precise control over material properties, thereby enabling the rational design and optimization of SnO2-doped TiO2 thin films for advanced functional applications.

Therefore, this research endeavours to address this specific knowledge

deficit. We systematically investigate the influence of varying SnO2 concentrations (0.0, 0.09, 0.9, and 9 at.%) and post-deposition annealing on the definitive crystalline structural parameters—including phase constitution, lattice constants, crystallite size, microstrain, dislocation density, and unit cell volume—as well as the fundamental optical properties of TiO2 thin films synthesized via the Spray Pyrolysis Technique. The objective is to provide crucial insights into how SnO2 doping, coupled with thermal treatment, can be strategically employed to tailor the functional characteristics of TiO2 thin films.

2.0 EXPERIMENTAL DETAILS

2.1 Materials

Titanium butoxide [$Ti(OCH_2CH_2CH_2CH_3)_4$], with a concentration of 0.1 M, was the preliminary solution used to produce the pure TiO_2 thin film. The spray pyrolysis system used ferric chloride as the raw dopant chemical in the starting solution to obtain the SnO2-doped products. A small amount of hydrochloric acid (approximately 10 mL) was added to both solutions to achieve consistency. Accordingly, the spray solution contained SnO_2 concentrations of 0.0, 0.09, 0.9, and 9 at.%. The different doping ratios were obtained according to the models illustrated in Table 1. Deionized water was used in all cases in the current research.

Table 1: Details of the TiO2 doping percentage

Sample No.	TiO_2 Solution		SnO_2 Solution		Doping molar ratio
	Volume c.c	Concentration mol/L	Volume c.c	Concentration mol/L (10^{-4})	
1	10	0.12515	……	…….	Pure
2	10	0.12515	90	1.12275	1:0009
3	10	0.12515	90	11.2275	1:009
4	10	0.12515	90	112.275	1:09

2.2 Synthesis of TiO_2 thin films

In thermal chemical spraying pyrolysis techniques, the material to be deposited as a liquid is placed inside a solution cylinder. The powder of TiO_2 with a purity of 97.0% was purchased from Sigma-Aldrich, and SnO2 powder with a purity of 99.9% was purchased from SkySpring Nanomaterials, Inc. The TiO_2 powder was dissolved in 10 mL of concentrated hydrochloric acid, mixed using a magnetic stirrer,

and heated at 50°C for 1 hour. As a result, the transparent solution was diluted with distilled water to obtain a stock solution. For SnO_2 doping, the powder was dissolved in 10 mL of concentrated hydrochloric acid for 15 minutes. The resulting solution was diluted with distilled water.

The sedimentation rate was 2.25 ml/min, and the normal distance between the spray nozzle and the glass substrate was 30-33 cm. The spraying time was 30 seconds, with an interval of 60 seconds. A closed or open reactor is then used, and gases are passed over it for reaction or carried as a spray to move through the reactor. The substance is then deposited from the vapor phase onto heated substrates. The system used to prepare the films consists of the following parts, as shown in Figure 1. The head of the spraying unit consists of a glass capillary tube connected at the upper end to a solution cylinder via a glass valve and at the lower end to a gradually reduced diameter, forming the spray nozzle, surrounded by a spherical glass capillary connected to an air pressure pump.

Air is compressed through a network of pipes inside the drying furnace. This step aims to prevent the shattering of glass substrates due to thermal shock. The glass substrate heater primarily consists of a resistive thermal wire covered by a stainless-steel plate, on which the substrates are placed. The temperature is measured using a thermocouple, which is connected to a digital controller. The coating was applied to glass strips ($75 \times 25 \times 1$ mm^3). The temperature of the glass substrates was maintained at 450°C to achieve a thin layer with a thickness of approximately 0.12 μm. After deposition, the pure TiO_2 and doped TiO_2 with 9% SnO_2 were subjected to annealing in air at 250°C and 450°C for 90 minutes. This annealing process was conducted to investigate and reflect the impact of thermal treatment on the optical properties of the TiO_2 thin film.

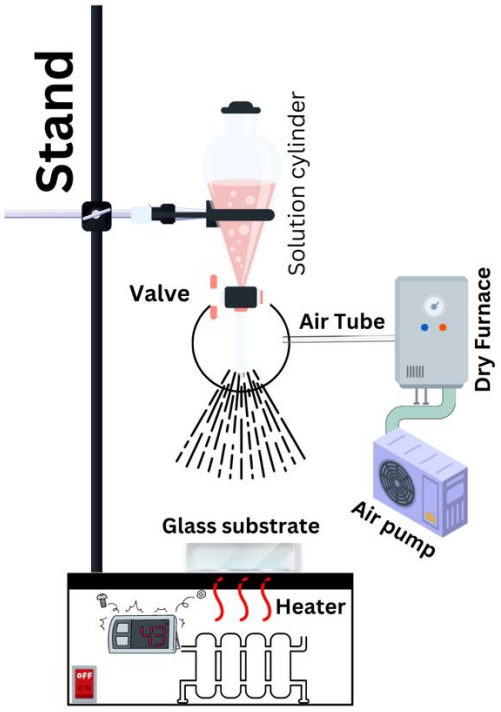

Figure 1: Experimental setup of the spray pyrolysis technique.

The hydrolysis of metal alkoxides has been followed by the formation of particles of metal oxide (TiO2). To produce a thin layer of TiO2, the following reaction can occur on a heated substrate: Ti (IV)-butoxide as a precursor and water as a reactant. Hydrolysis of Titanium Alkoxide [28]:

$$Ti[OCH(CH_3)_2]_4 + 4H_2O \rightarrow Ti(OH)_4 + 4C_3H_7OH \quad (1)$$

Hydrolysis of Tin(IV) Chloride:

$$SnCl_4 + 4H_2O \rightarrow Sn(OH)_4 + 4HCl \quad (2)$$

The possible chemical reactions during forming of SnO2-doped TiO2 thin films, possibly with Sn^{4+} ions incorporated into the TiO_2 lattice, are given as:

$$Ti(OH)_4 + Sn(OH)_4 \rightarrow TiO_2 \cdot SnO_2 + 4H_2O \quad (3)$$

2.3 Thin film characterization techniques

Pure TiO2 and doped thin films were used to examine structural and optical properties using various instrumental techniques. The crystallinity and phase identification analysis were performed using a Shimadzu-6000 X-ray diffractometer equipped with a nickel filter, employing monochromatic CuKα radiation at 40 kV and 30 mA to determine the crystal structure of the films. The films were scanned at 2° per minute, with a scanning range of 20 ° to 60 °. Based on the XRD results, the crystal structure parameters were examined by calculating the lattice constants a and c, crystal volume D, dislocation density δ, internal strains ε, unit cell volume (V), and thin film density (ζcaI). The relationship calculates the lattice constants for the produced thin films [27]:

$$\frac{1}{d^2} = \frac{(h^2+k^2)}{a^2} + \frac{I^2}{c^2} \quad (4)$$

Where d is the distance between adjacent planes in the group, (h, k, l) are Miller's indices, and a and c are the lattice parameters (in a tetragonal system). The crystal size is calculated from the Debye-Scherrer formula [29, 30]:

$$D = \frac{k.\lambda}{\beta.cos\theta} \quad (5)$$

In the above equation, K is the Scherrer constant equal to 0.94, λ is the wavelength, β is the full width at half maximum (FWHM), and θ is the Bragg angle. The dislocation density (δ) of the crystal volume (D) can be calculated by the relationship [31]:

$$\delta = \frac{1}{D^2} \quad (6)$$

The microstrain (ε) of the prepared pure and doped TiO2: SnO2 thin films can be calculated based on the Williamson-Hall technique using the following equation [32]:

$$\varepsilon = \frac{\beta}{4\times tan\theta} \quad (7)$$

Where β is the full width at half maximum, and θ is the Bragg angle. The unit cell volume and density for a crystal structure of the bare and doped TiO2 thin films can be calculated using the following formula:

$$V = a^2 \cdot c$$

$$\zeta caI = \frac{(M_W \times Z \times 1.66)}{V} \quad (8)$$

Based on the above relations, Mw is the molecular weight (mol/g), Z is the number of formula units per unit cell, and 1.66 is a conversion factor. Using a PerkinElmer (Lambda-950) UV-visible-near infrared spectrometer with an integrating sphere, the optical properties were determined using UV-visible spectroscopy ranging from 100 to 1200 nm.

3.0 RESULTS AND DISCUSSION

3.1 Microstructural investigations

Figure 2 displays the XRD patterns of pure and doped Ti O_2 thin film samples with 9 at.% SnO_2 with and without annealing. The Results revealed that the XRD peaks confirmed the anatase phase of a tetragonal crystal arrangement in the pure sample, having a space group of I41/amd (JCPDS 21–1272) (Weng et al., 2005). A high-intensity peak indicates good crystallinity of the TiO2 nanoparticles. It was found that the anatase phase transformed to the rutile phase after adding SnO2; however, the intensity of this phase decreased after the annealing treatment. A comparative analysis in Table 2 reveals the standard and synthesized TiO_2, showing subtle but significant differences in lattice parameters, unit cell volume, and density, which can profoundly influence the material's properties. Both the standard TiO_2 and the TiO_2 from the present study exhibit a tetragonal crystal structure characteristic of the anatase phase of TiO_2. However, a closer examination of the lattice parameters reveals a slight reduction in the present study's values of (a) and (c).

Specifically, the lattice parameter (a) decreases from 3.7852 Å in the standard TiO_2 to 3.77816 Å in the synthesized sample, while the lattice parameter (c) decreases from 9.5139 Å to 9.44128 Å. Consequently, the unit cell volume (V) also reduces from 136.31 $Å^3$ to 134.769 $Å^3$. Therefore, the contraction of the unit cell dimensions suggests that the TiO_2 analyzed here might be under compressive strain or that changes in synthesis conditions at some purity level affected the crystal structure. The lattice parameter and unit cell volume would thus correspond to changes in density. The density (ζcal) of the TiO_2 thin film in the present study is calculated to be 3.921037 g/cm^3, which is slightly higher than the standard density of TiO_2, 3.892 g/cm^3. This increase in density could indicate a more compact atomic arrangement within the unit cell or a reduction in porosity, leading to a denser

material. The higher density is consistent with the observed decrease in lattice parameters, as the atoms in the unit cell are more closely packed.

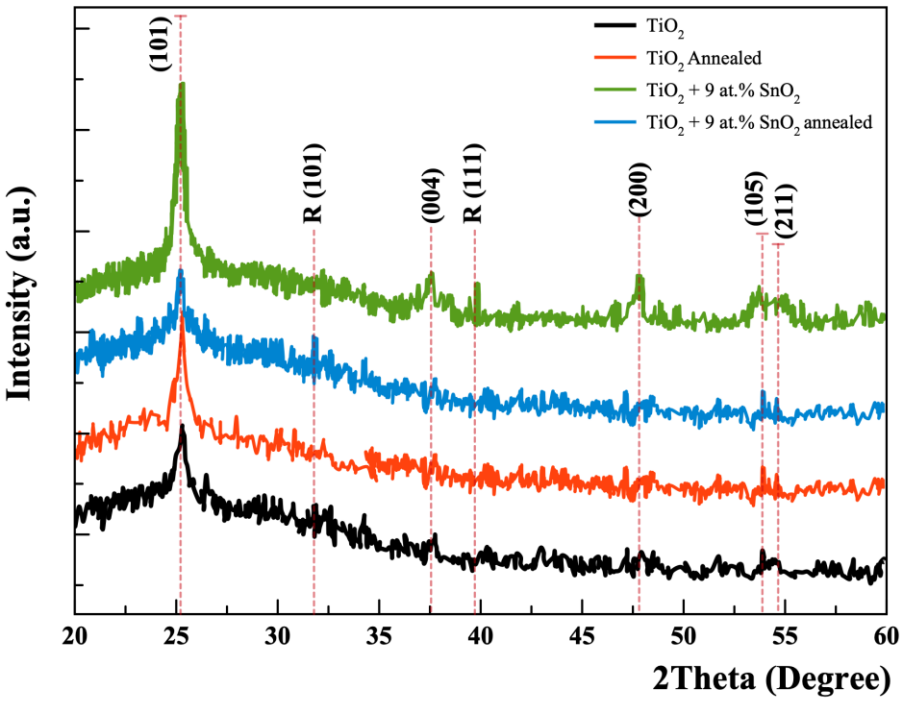

Figure 2. XRD spectra of bare and SnO2-doped, and annealed TiO2 thin films.

Table 2: Comparison of structural parameters of the TiO2 standard and the current study.

TiO_2 Present Study				TiO_2 Standard			
NO.	θ2	dA°	I/Io	θ2	dA°	I/Io	(hkl)
1	25.3005	3.51737	100	25.281	3.5200	100	101
2	38.0953	2.36032	24	37.800	2.3780	20	004
3	48.1291	1.88908	12	48.049	1.8920	35	200
4	53.4667	1.71239	8	53.890	1.6999	20	105
5	55.1861	1.66304	8	55.060	1.6665	20	211

System: Tetragonal a= 3.77816 A° c= 9.44128 A° Vo= 134.769 A° z= 4β Mw= 79.9 ζcaI= 3.921037 g/cc	System: Tetragonal a = 3.7852 A° c= 9.5139 A° Vo= 136.31 A ° z= 4β Mw= 79.9 ζcaI= 3.892 g/cc

Table 3 shows the key parameters observed, including density (ζcaI), crystallite size (δ), strain (ε), and dislocation density (D), to declare the effect of annealing and doping on the crystal of the TiO2 thin film. Firstly, the density of TiO_2 increases significantly to 4.19906 g/cc when doped with 9 at.% SnO_2. This increase suggests that incorporating SnO_2 into the TiO_2 matrix results in a denser or more compact structure. When TiO_2 is annealed without doping, the density slightly increases to 3.9366 g/cc, suggesting that annealing alone also contributes to a denser material, possibly by reducing defects or porosity. However, in the case of the doped and annealed TiO_2, the density slightly decreases to 4.17403 g/cc compared to the non-annealed doped sample, implying that annealing may slightly counterbalance the densifying effect of doping, potentially due to changes in the microstructure that reduce overall material compactness. Encompassing dopants can lead to structural changes in TiO2, affecting crystallization density. The crystallite size (δ) with the doping of SnO_2 reduces this size to 0.24 x 10^{-4} $A°^{-2}$, indicating that the presence of SnO_2 leads to a refinement of the crystal grains.

Annealing the pure TiO_2 further reduces the crystallite size to 0.158 × 10^{-4} $A°^{-2}$, indicating that the heat treatment process promotes the formation of smaller, more uniform grains. The smallest crystallite size, 0.097 x 10^{-4} $A°^{-2}$, is observed in the annealed and doped TiO_2. This implies that simultaneous doping and annealing lead to the formation of an intended crystal structure, which, in turn, enhances the mechanical and optical properties of the material, as a larger number of grain boundaries will now be involved. Xue et al. (2020) quantified that high-level molybdenum doping caused lattice distortion, acting as a barrier to grain growth and suppressing the anatase-to-rutile phase transformation [33]. This is very important since the phase composition of TiO2 plays a critical role in its photocatalytic performance. Doping processes result in structural defects that may hinder crystallization. In the process of doping with nitrogen, for instance, the nitrogen atoms are accommodated within the matrix. Such a process leads to lower

crystallinity and higher amorphous phases within the TiO2 structure [34, 35].

As doped materials may have the propensity to affect crystallization density, determining possible changes in thermal stability is also essential. According to their study, Kumaravel et al. (2021) introduced tantalum doping, which demonstrates that TiO2 is more thermally stable while simultaneously reducing the average crystallite size [36]. Thus, doping concentration, crystallization density, and thermal property have established a multidimensional relationship. It is also of significant interest to many applications that require high thermal stability, including solar cell-related technologies. Besides, aluminum tends to change the crystalline structure and surface roughness of TiO2 during doping. Changes in crystallization density are related to higher surface roughness values [37, 38]. This implies that aluminum can also act bimodally, allowing structural and electronic properties to change and endowing new functionalities on TiO2.

Table 3: Variation of density (ζcaI), the crystallite size (δ), strain (ε), and dislocation density (D) of pure, doped, and annealed TiO2 thin films.

Sample	2θ	D(A°)	(hkl)	a (A°)	c (A°)	β degree	D(A°)	$A^{\circ-2}\,\delta$ x 10^{-4}	ε x 10^{-4}	ζcaI (g/cc)
TiO_2 Pure	25.3005	3.51737	(101)	3.77816	9.44128	0.4915	173.02	0.334	2.477	3.9210
TiO_2 + 9 at.% SnO2	25.2752	3.523		3.77372	9.5795	0.5166	204.106	0.24	2.076	4.19906
TiO_2 annealed	25.3171	3.5151		3.77816	9.4788	0.3381	251.547	0.158	1.682	3.9366
TiO_2 + 9 at.% SnO2 annealed	25.2558	3.52349		3.79646	9.52183	0.2651	320.749	0.097	1.349	4.17403

Pure TiO_2 doped with 9 at.% SnO_2 results in a further decrease in microstrain, down to 2.076 x 10^{-4}, while doping relaxes part of the

internal stress in the host material. On the other hand, annealing treatment on pure TiO_2 reduced strain to 1.682 x 10^{-4}, suggesting that thermal treatment relaxed the crystalline structure by releasing part of the stress. The least strain recorded, 1.349 x 10^{-4}, was caused by the combined effect of doping and annealing. This observation indicates that when doping is applied successively, followed by annealing, maximum relaxation occurs within the crystal lattice, making the material more stable and less mechanically stressed. The incorporation of non-metal dopants, such as nitrogen, has been widely studied. In this respect, it has been reported that the incorporation of nitrogen into TiO_2 reduces its bandgap, hence increasing its absorbance within the visible light spectrum. The electronic structure may also influence microstrain, as the incorporation of nitrogen can lead to changes in interplanar spacing, which consequently affect the overall crystallinity of the films. Other defects can also be induced, particularly during the crystallization process, which, in turn, promotes further micro-strain and, hence, negatively affects the film's mechanical stability. Gd doping of TiO_2 established that micro-strain was d-level dependent and could be minimized under proper doping conditions, resulting in improved structural properties without excess strain that could lead to potential delamination or cracking. Similarly, at higher dopant concentrations, the dislocation densities and microstrain of the TiO_2 thin films are said to compromise their structural stability. For pure TiO_2, a dislocation density that was increasing to 204.106 A° with doping population did not show any plateau, suggesting that either doping introduces new dislocations or amplifies the existing ones, which perhaps contributes to the overall strengthening. Further annealing of pure TiO_2 increased the dislocation density to 251.547 A°, indicating that the annealing procedure provides strain relief, but possibly introduces additional dislocations. The most considerable amount, 320.749 A°, was observed for the sample that underwent simultaneous annealing and doping. That may indicate that such combined processes lead to a greater breakage of the crystal structure, thereby hardening it with increased brittleness. Eskalen and Kerli (2020) demonstrated that Gd doping alters the optical bandgap while enhancing pollutant photocatalytic degradation, which may be related to changes in dislocation density [39]. The structural characterization of the films revealed differences in crystallite size and microstrains in the doped samples, which are attributed to the origin of dislocation density. Doping concentration has a complex relationship with dislocation density, as high doping levels can increase lattice distortion, leading to a higher dislocation density.

The influence of nitrogen (N) doping on the properties of TiO_2 thin films has been extensively studied. It was reported that N-doping enhanced visible light absorption and photocatalytic activity, which were linked to changes in the thin film's dislocation density [40]. Therefore, integrating nitrogen into the TiO_2 lattice may introduce additional defects, increasing dislocation density and affecting the overall structural properties of the thin films.

3.2 Optical properties

Figure 3 shows the optical transmittance properties for SnO_2-doped and bare TiO_2 thin films at different SnO_2 doping concentrations. Pure TiO_2 is transparent; in fact, it exhibits high transmittance throughout the visible and near-infrared regions, approximately within the wavelength range of 400 nm to 1100 nm, with transmittance values above 60%. The TiO_2 thin film typically exhibits a high level of transparency, making it a suitable material for applications that require transparent or clear substances. SnO_2 doping into the TiO_2 matrix significantly influences their transmittance in a concentration-dependent manner.

The orange curve represents the sample with 0.09% SnO_2 doping, showing that the light transmittance in the visible and NIR regions decreases slightly compared to that of pure TiO_2. That is, doping affects the material's optical transparency in small percentages, likely due to the addition of extra scattering centers or absorption processes associated with the SnO_2 dopant. A drastic decrease in transmittance occurs at a 0.9% SnO_2 concentration. The test sample exhibits relatively poor transmittance across the spectrum, characterized by significant loss in the visible region. The reduction in transparency is likely due to the increased concentration of SnO_2, which likely creates more scattering centers or enhances absorption, thereby reducing the amount of light that can be transmitted through the material.

This is most pronounced in the sample doped with 9% SnO_2; however, the transmittance is considerably lowered across the measured wavelength range and even falls below 20% in both the visible and NIR regions. A significant decrease in transparency across this range indicates that the high addition of SnO_2 results in a highly nontransparent material. The addition of SnO2 to TiO2 thin films has been found to affect the properties relating to transmittance. The reduction of the energy band gap of TiO2, upon incorporating SnO2,

has been observed in TiO2, which involves the optical transmittance. This is associated with the presence of intermediate energy states between the band gaps, which facilitate electron transitions, and thus, changes such as material absorption occur [41-43]. These results confirm that the optical bandgap of the composite material decreases from ~3.64 eV to ~3.57 eV by increasing the SnO2 concentration, thereby causing a significant increase in absorbance at specific wavelengths in the primarily ultraviolet regions of the spectrum [44].

Additionally, the optical properties of modifying SnO2 thin films by doping with various elements have been extensively studied. For instance, the transmittance of SnO2 films decreases with increasing doping concentration, indicating an optimal balance between doping level and optical absorption [45, 46]. This can be taken to mean that although doping might enhance specific properties, it is also likely to generate defects with light absorption capabilities.

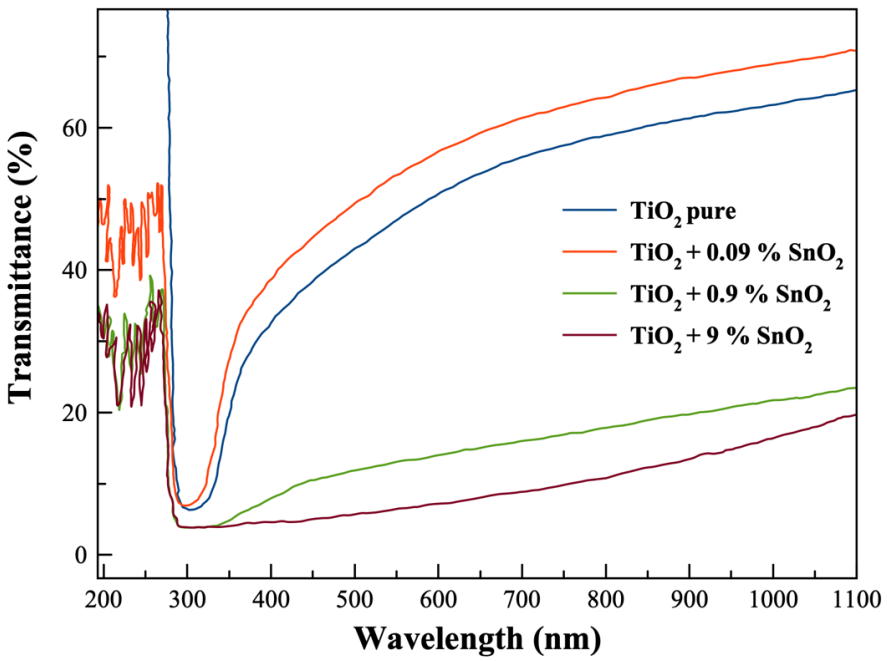

Figure 3. The optical transmittance of TiO_2 thin films doped with different percentages of SnO_2.

Figure 4 shows the absorption features of materials that reveal how different doping concentrations of SnO_2 change the optical properties of the host material TiO_2. Such behavior is of utmost importance when designing a material with a specific application in mind, such as

regulating light absorption in solar photovoltaics, sensors, and optical coatings. In other words, the nature of the absorbance- the amount of light absorbed by it through which the wavelength of light has to pass- shows a direct relationship to its applicability in technological and industrial areas. The absorbance profile of virgin TiO_2 is defined by a characteristic profile with one central UV peak centered at 300 nm. This peak, present at an absorbance of just over 2.5%, indicates the strong ability of a TiO_2 thin film to absorb UV light. This is a direct result of the wide band gap of TiO_2, which effectively hosts high-energy UV photons. Absorbance behavior has been slightly different in TiO_2 doped with 0.09%. The peak absorbance in the UV region remains, albeit somewhat lower than that of pure TiO_2; thus, the reduction in UV absorption is marginal. This suggests that the electronic structure of the material is moderately altered by the presence of even a small amount of SnO_2, either through a slight change in the bandgap or the introduction of new scattering centers, which decrease the total UV absorbance. With an increasing concentration of SnO_2, changes in absorbance became increasingly significant, reaching 0.9 at.% addition.

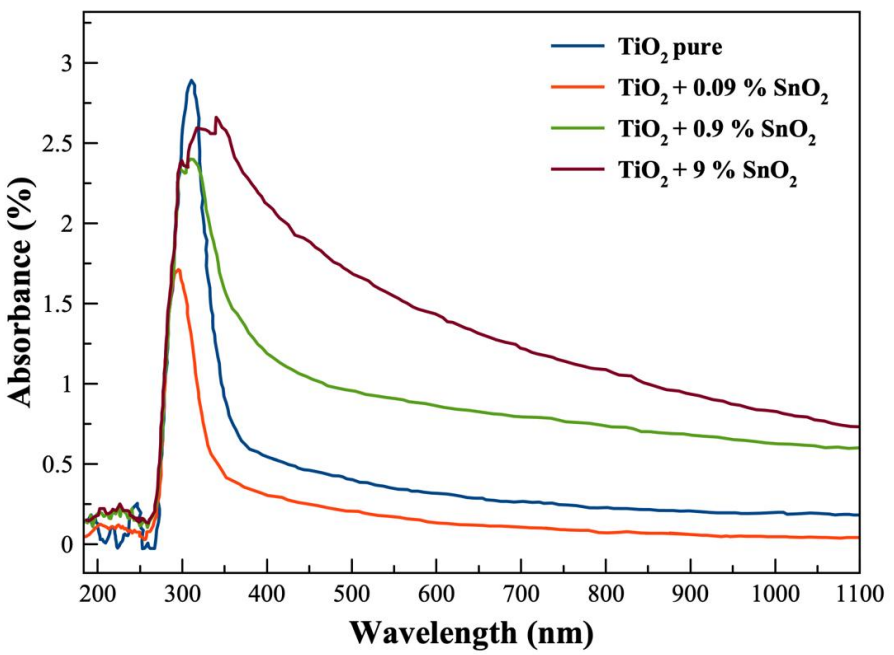

Figure 4. The optical absorbance of TiO_2 thin films doped with different percentages of SnO_2.

It also showed an absorbance peak in UV at 2% lower than the pure TiO_2 and 0.09% SnO_2-doped sample. This even lesser decrease in UV

absorbance now indicates that the modification in bandgap electronic structure is enhanced by the increase in SnO_2 doping or increased light scattering, which generally reduces the material's potential to absorb UV light. This can be easily seen from the absorption behavior for 9% SnO_2-concentrated solid solutions, for which this concentration was assumed to stabilize the practical photocatalytic applications of the rutile phase of TiO2 [47]. The increase in the crystallite size tends to enhance the light-scattering and absorption properties of the doped TiO2 films. By the effect of SnO2 in a proper way, the specific surface area of TiO2 films increased, which increases the potential of the pollutants' adsorption and promotes the photocatalytic efficiency of these materials [48, 49]. Figure 5 shows the transmittance percentage of TiO_2 doped with 9% SnO_2 after annealing at two different temperatures, 250°C and 450°C, over a wavelength range of 200 nm to 1000 nm.

Regarding the transmittance percentage of the sample in the wavelength range of 200-400 nm, the difference in the transmittance is not significant with respect to the annealing temperature. Therefore, the lower annealing temperature maintains some transmission in the ultraviolet range compared to the higher one. For the full spectrum, the transmittance of the specimen with the 250°C anneal is always higher than the one annealed at 450°C within the 400-1000 nm range. This tendency becomes more visible in the case of longer wavelengths because, for the annealed specimen, the transmittance constantly increases to over 30% compared with the specimen annealed at 450°C. It retains a relatively low level, below 30%, of transmittance. Therefore, higher annealing at 450°C results in lower overall transmittance compared with the 250°C-annealed specimen. At higher temperatures, increased grain growth defects or even a phase transition may occur within the TiO_2-SnO_2 matrix, impairing the material's optical transparency.

Annealing of TiO2 thin films at a moderate temperature, typically around 500 °C, has also been reported to improve optical transmittance. For instance, it has been demonstrated that TiO2 films exhibit an improvement in transmittance, increasing from approximately 45% in the as-deposited state to nearly 80% after annealing at 500 °C, particularly within the visible and near-infrared spectra [50]. The enhancements have been attributed to the improved crystallization and reduced scattering resulting from the densification of the films, thereby lowering the defects and surface roughness that

can scatter light [51, 52]. However, the gains that come with annealing plunge or even become null at high temperatures. Indeed, when the annealing temperature exceeds 500 °C, most of the transmission drops to very low numbers. This can be attributed to the creation of oxygen vacancies and increased surface roughness, which may enhance light scattering [51]. These have been noted by authors to be responsible, in turn, for diminishing optical transmittance when the annealing temperature exceeds 300 °C. Another aspect is that while the amorphous-to-crystalline phase transformation, and especially the appearance of the anatase phase, can improve transmittance at the initial stage, with increasing temperatures, absorptance rises, along with modifications in grain size and structure [50, 52].

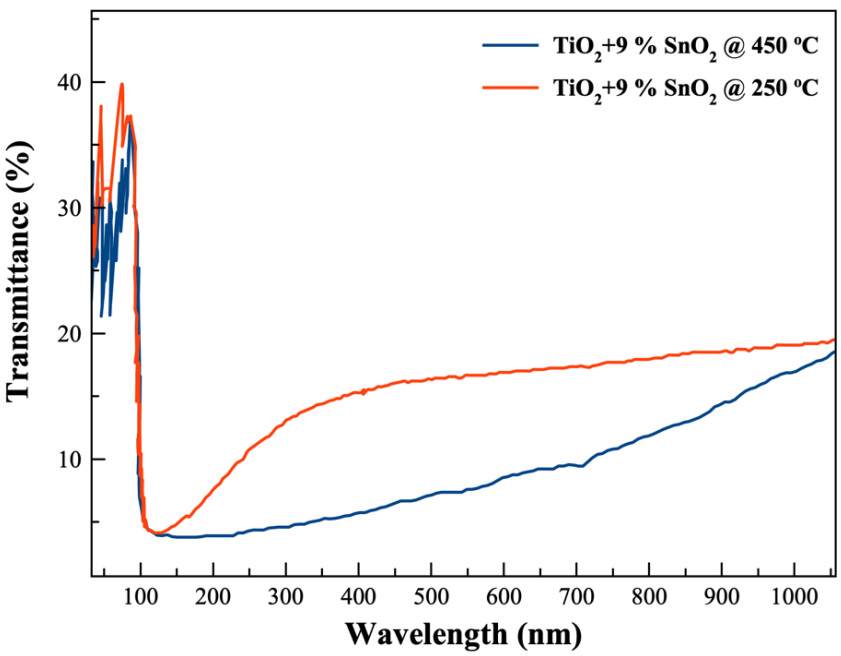

Figure 5. The optical transmittance of doped TiO2 thin films subjected to 250°C and 450°C for 90 min.

Figure 6 shows the absorbance for TiO_2 doped with 9% SnO_2 at annealing temperatures of 250 °C and 450 °C. It was found that a considerable absorbance peak exists in the UV region, corresponding to TiO_2, which intrinsically absorbs high energy at UV wavelengths. In contrast, the sample annealed at 450°C shows a higher peak absorption, just above 2.5%, while the 250°C-annealed sample peaked at about 1.7%. The result of higher absorbance at 450°C suggests that higher-temperature annealing may increase the material's capability to absorb

ultraviolet light, either due to increased crystallinity or reduced defects, or by altering the electronic structure in favor of more efficient light absorption. The absorbance for both samples gradually decays with increasing wavelength in the visible and NIR regions.

On the other hand, the sample annealed at 450°C systematically shows higher absorbance than the sample annealed at 250°C in the same region. In the visible region, the absorbance of the sample annealed at 450°C is much higher, reflecting that the sample will absorb more light and, hence, be less transparent. Higher annealing temperatures have been shown to increase the material's crystallinity, which is related to stronger electronic interactions among the thin film particles [53]. This improvement in crystallinity is essential, as it can potentially reduce defects and oxygen vacancies, which are known to affect the absorption properties of the films [54]. A shift of the absorption edge of Ni-doped TiO2 thin films to the visible range has been observed with increased annealing temperature. This denotes a change in the electronic structure of the films. Dussan et al. (2017) noted that the morphology of most TiO2 films is primarily influenced by the annealing process, which modifies their absorption characteristics, in addition to other properties [55]. Indeed, the results of Daamouche and Guitoume (2023) confirm that the improvement in the structural integrity of TiO2 thin films at an elevated annealing temperature enhances their properties, which in turn explains their optical characteristics [56].

The relationship between film morphology and optical absorption is quite complex; changes in surface roughness can affect grain size, which in turn relates to light-scattering and absorption efficiencies.

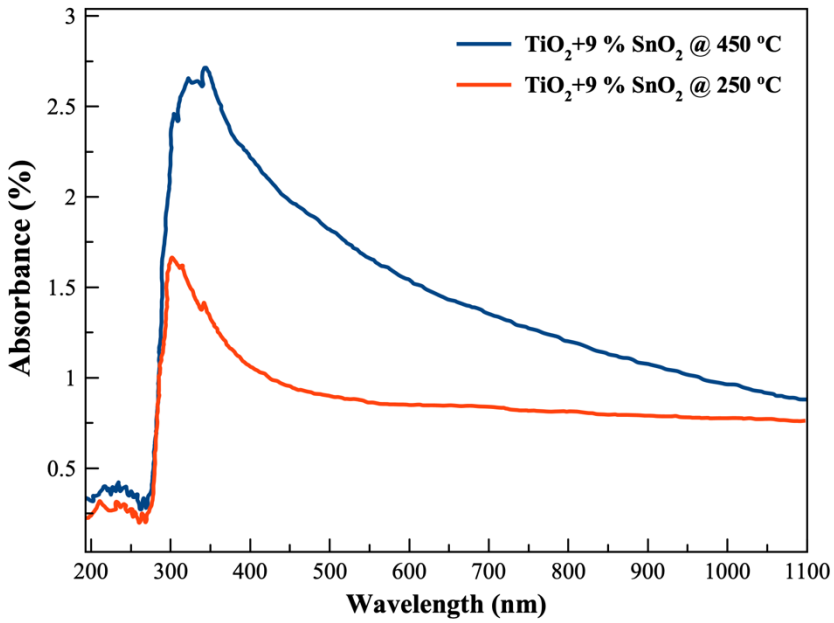

Figure 6. The optical absorbance of doped TiO2 thin film subjected to 250 °C and 450 °C for 90 min.

4.0 CONCLUSION

In conclusion, this study has demonstrated that the addition of SnO_2 and subsequent annealing treatments have a significant impact on the structural and optical properties of TiO_2 thin films. The transformation from the anatase to the rutile phase, observed with increasing SnO_2 concentration, highlights the doping effect on the crystalline structure of TiO_2. XRD analyses of the doped films revealed a reduction in lattice parameters and, consequently, a decrease in unit cell volume, indicating an increase in material density. Furthermore, after annealing, the crystalline size and microstrain of the doped films decreased, suggesting enhanced material stability. SnO_2 doping resulted in a significant reduction in transmittance and an increase in absorbance, particularly at higher doping levels, as indicated by the optical characteristics. This effect was more pronounced in films annealed at higher temperatures, suggesting that doping and annealing processes can be controlled to achieve specific optical

responses. Additionally, the decrease in the energy band gap due to SnO_2 doping supports the potential use of tailored TiO_2 films in applications where precise control of optical properties is required.

ACKNOWLEDGMENTS

The authors would like to sincerely thank the University of Babylon for providing the necessary resources and support throughout the research process.

AUTHOR CONTRIBUTIONS

M.M.A. Alhaffar: Conceptualization, Methodology, Software, Writing - Original Draft Preparation; F.K. Dahash: Software, Validation, Writing - Reviewing and Editing; S.N.S. Al-Humairi: Writing - Reviewing and Editing; M.H. Almaamori: Data Curation, Validation, Supervision.

CONFLICTS OF INTEREST

The manuscript has not been published elsewhere and is not under consideration by any other journals. All authors have approved the review, agree with its submission, and declare no conflict of interest in the manuscript.

REFERENCES

[1] D. K. Baisnab, S. Mukherjee, and S. Das, "A short review on inorganic thin films from device perspective", in *Chemical Solution Synthesis for Materials Design and Thin Film Device Applications*, 2021, pp. 231-275.

[2] O. A. Jassim, M. M. Mutter, and S. Khalil, "Effect of Al-Doped on the Electrical Properties of Nb2O5 Film Prepared by DC. Plasma Sputtering Technique," in *Materials Science Forum*, vol. 1050, Trans Tech Publ, 2022, pp. 21-33.

[3] X. Chen and S. S. Mao, "Titanium dioxide nanomaterials: synthesis, properties, modifications, and applications", *Chemical Reviews*, vol. 107, no. 7, pp. 2891-2959, 2007.

[4] S. Lettieri, M. Pavone, A. Fioravanti, L. Santamaria Amato, and P. Maddalena, "Charge carrier processes and optical properties in TiO2 and TiO2-based heterojunction photocatalysts: A review", *Materials*, vol. 14, no. 7, p. 1645, 2021.

[5] D. Reyes-Coronado, G. Rodríguez-Gattorno, M. Espinosa-Pesqueira, C. Cab, R. De Coss, and G. Oskam, "Phase-pure TiO2 nanoparticles: anatase, brookite and rutile", *Nanotechnology*, vol. 19, no. 14, p. 145605, 2008.

[6] D. R. Eddy, M. D. Permana, L. K. Sakti, G. A. N. Sheha, Solihudin, S. Hidayat, T. Takei, N. Kumada, and I. Rahayu, "Heterophase polymorph of TiO2 (Anatase, Rutile, Brookite, TiO2 (B)) for efficient photocatalyst: fabrication and activity", *Nanomaterials*, vol. 13, no. 4, p. 704, 2023.

[7] H.-R. An, S. Y. Park, H. Kim, C. Y. Lee, S. Choi, S. C. Lee, S. Seo, E. C. Park, Y.-K. Oh, C.-G. Song, J. Won, Y. J. Kim, J. Lee, H. U. Lee, and Y.-C. Lee, "Advanced nanoporous TiO2 photocatalysts by hydrogen plasma for efficient solar-light photocatalytic application", *Scientific Reports*, vol. 6, no. 1, p. 29683, 2016.

[8] M. Kapilashrami, Y. Zhang, Y.-S. Liu, A. Hagfeldt, and J. Guo, "Probing the optical property and electronic structure of TiO2 nanomaterials for renewable energy applications", *Chemical Reviews*, vol. 114, no. 19, pp. 9662-9707, 2014.

[9] M. Al-Mamun, S. Kader, M. Islam, and M. Khan, "Photocatalytic activity improvement and application of UV-TiO2 photocatalysis in textile wastewater treatment: A review", *Journal of Environmental Chemical Engineering*, vol. 7, no. 5, p. 103248, 2019.

[10] J. P. Jeon, D. H. Kweon, B. J. Jang, M. J. Ju, and J. B. Baek, "Enhancing the photocatalytic activity of TiO2 catalysts", *Advanced Sustainable Systems*, vol. 4, no. 12, p. 2000197, 2020.

[11] C. P. M. de Oliveira, I. F. Farah, K. Koch, J. E. Drewes, M. M. Viana, and M. C. S. Amaral, "TiO2-Graphene oxide nanocomposite membranes: A review", *Separation and Purification Technology*, vol. 280, p. 119836, 2022.

[12] M. N. Chaudhari, R. B. Ahirrao, and S. D. Bagul, "Thin film deposition methods: A critical review", *International Journal for Research in Applied Science and Engineering Technology*, vol. 9, no. 6, pp. 5215-5232, 2021.

[13] D. Lundin and K. Sarakinos, "An introduction to thin film processing using high-power impulse magnetron sputtering", *Journal of Materials Research*, vol. 27, no. 5, pp. 780-792, 2012.

[14] H.-U. Krebs, M. Weisheit, J. Faupel, E. Süske, T. Scharf, C. Fuhse, M. Störmer, K. Sturm, and M. Seibt, "Pulsed laser deposition (PLD)--a versatile thin film technique", in *Advances in Solid State Physics*, Springer, 2003, pp. 505-518.

[15] K. B. Masood, P. Kumar, M. A. Malik, and J. Singh, "A comprehensive tutorial on the pulsed laser deposition technique and developments in the fabrication of low dimensional systems and nanostructures", *Emergent Materials*, vol. 4, no. 3, pp. 737-754, 2021.

[16] L. Filipovic, S. Selberherr, G. C. Mutinati, E. Brunet, S. Steinhauer, A. Köck, J. Teva, J. Kraft, J. Siegert, and F. Schrank, "Methods of simulating thin film deposition using spray pyrolysis techniques", *Microelectronic Engineering*, vol. 117, pp. 57-66, 2014.

[17] S. R. Sriram, S. R. Parne, N. Pothukanuri, and D. R. Edla, "Prospects of spray pyrolysis technique for gas sensor applications–A comprehensive review", *Journal of Analytical and Applied Pyrolysis*, vol. 164, p. 105527, 2022.

[18] M. Sahal, B. Hartiti, A. Ridah, M. Mollar, and B. Marí, "Structural, electrical and optical properties of ZnO thin films deposited by sol–gel method", *Microelectronics Journal*, vol. 39, no. 12, pp. 1425-1428, 2008.

[19] M. Ortega-López, A. Avila-García, M. Albor-Aguilera, and V. S. Resendiz, "Improved efficiency of the chemical bath deposition method during growth of ZnO thin films", *Materials Research Bulletin*, vol. 38, no. 7, pp. 1241-1248, 2003.

[20] F. G. Hone, F. K. Ampong, T. Abza, I. Nkrumah, R. K. Nkum, and F. Boakye, "Investigating the effect of deposition time on the morphology, structure and optical band gap of PbS thin films synthesized by CBD technique", *Elixir Thin Film Tech*, vol. 76, pp. 28432-28437, 2014.

[21] R. S. Kate, H. M. Pathan, R. Kalubarme, B. B. Kale, and R. J. Deokate, "Spray pyrolysis: Approaches for nanostructured metal oxide films in energy storage application", *Journal of Energy Storage*, vol. 54, p. 105387, 2022.

[22] P. Patil and L. Kadam, "Preparation and characterization of spray pyrolyzed nickel oxide (NiO) thin films", *Applied Surface Science*, vol. 199, no. 1-4, pp. 211-221, 2002.

[23] W. Naffouti, A. Jrad, T. Ben Nasr, S. Ammar, and N. Turki-Kamoun, "Structural, morphological and optical properties of TiO2: Mn thin films prepared by spray pyrolysis technique", *Journal of Materials Science: Materials in Electronics*, vol. 27, pp. 4622-4630, 2016.

[24] L. Patil, D. Suryawanshi, I. Pathan, and D. Patil, "Nickel doped spray pyrolyzed nanostructured TiO2 thin films for LPG gas sensing", *Sensors and Actuators B: Chemical*, vol. 176, pp. 514-521, 2013.

[25] F. Huang, Q. Li, G. J. Thorogood, Y.-B. Cheng, and R. A. Caruso, "Zn-doped TiO2 electrodes in dye-sensitized solar cells for enhanced photocurrent", *Journal of Materials Chemistry*, vol. 22, no. 33, pp. 17128-17132, 2012.

[26] M. Sreedhar, I. N. Reddy, C. V. Reddy, J. Shim, and J. Brijitta, "Highly photostable Zn-doped TiO2 thin film nanostructures for enhanced dye degradation deposited by sputtering method", *Materials Science in Semiconductor Processing*, vol. 85, pp. 113-121, 2018.

[27] A. Arunachalam, S. Dhanapandian, C. Manoharan, and G. Sivakumar, "Physical properties of Zn doped TiO2 thin films with spray pyrolysis technique and its effects in antibacterial activity", *Spectrochimica Acta Part A: Molecular and Biomolecular Spectroscopy*, vol. 138, pp. 105-112, 2015.

[28] T. C. Paul, J. Podder, and L. Paik, "Effect of Fe doping on the microstructure, optical and dispersion energy characteristics of TiO2 thin films prepared via spray pyrolysis technique", *Results in Optics*, vol. 8, p. 100235, 2022.

[29] J. G. Mahy, R. G. Tilkin, S. Douven, and S. D. Lambert, "TiO2 nanocrystallites photocatalysts modified with metallic species: Comparison between Cu and Pt doping", *Surfaces and Interfaces*, vol. 17, p. 100366, 2019.

[30] T. C. Paul, J. Podder, and M. H. Babu, "Optical constants and dispersion energy parameters of Zn-doped TiO2 thin films prepared by spray pyrolysis technique", *Surfaces and Interfaces*, vol. 21, p. 100725, 2020.

[31] S. Dhanapandian, A. Arunachalam, and C. Manoharan, "Effect of deposition parameters on the properties of TiO2 thin films prepared by spray pyrolysis", *Journal of Sol-Gel Science and Technology*, vol. 77, pp. 119-135, 2016.

[32] R. Vidhya, M. Sankareswari, and K. Neyvasagam, "Effect of annealing temperature on structural and optical properties of Cu-TiO2 thin film", *Relation*, vol. 2, no. 1, pp. 1-5, 2016.

[33] D. Xue, J. Luo, Z. Li, Y. Yin, and J. Shen, "Enhanced photoelectrochemical properties from Mo-doped TiO2 nanotube arrays film", *Coatings*, vol. 10, no. 1, p. 75, 2020.

[34] S. Z. Islam and S. E. Rankin, "Hydrazine-based synergistic Ti (III)/N doping of surfactant-templated TiO2 thin films for enhanced visible light photocatalysis", *Materials Chemistry and Physics*, vol. 182, pp. 382-393, 2016.

[35] A. Aijaz, Y.-X. Ji, J. Montero, G. A. Niklasson, C. G. Granqvist, and T. Kubart, "Low-temperature synthesis of thermochromic vanadium dioxide thin films by reactive high power impulse magnetron sputtering", *Solar Energy Materials and Solar Cells*, vol. 149, pp. 137-144, 2016.

[36] V. Kumaravel, M. B. MacCioni, S. Mathew, S. J. Hinder, J. Bartlett, M. Nolan, and S. C. Pillai, "Unravelling the impact of Ta doping on the electronic and structural properties of titania: A combined theoretical and experimental approach", *The Journal of Physical Chemistry C*, vol. 126, no. 4, pp. 2285-2297, 2022.

[37] K. H. Rahman and A. K. Kar, "Effect of precursor concentration of microstructured titanium-di-oxide (TiO2) thin films and their

photocatalytic activity", *Materials Research Express*, vol. 6, no. 9, p. 096436, 2019.

[38] S. B. Nair, H. Rahman, J. A. Joseph, S. K. Remillard, and R. R. Philip, "Aluminium doping–a cost effective and super-fast method for low temperature crystallization of TiO2 nanotubes", *CrystEngComm*, vol. 21, no. 1, pp. 128-134, 2019.

[39] H. Eskalen and S. Kerli, "Synthesis of Gd doped TiO2 thin film for photocatalytic degradation of malachite green", *Sakarya University Journal of Science*, vol. 24, no. 6, pp. 1210-1215, 2020.

[40] A. Aijaz, Z. Uddin, and I. A. Siddiqui, "Structural Properties of Nitrogen Doped Anatase and Rutile TiO2 Thin Films", *Journal of Advances in Physics*, vol. 8, no. 2, pp. 2074-2078, 2015.

[41] N. Serpone, A. V. Emeline, V. N. Kuznetsov, and V. K. Ryabchuk, "Second generation visible-light-active photocatalysts: preparation, optical properties, and consequences of dopants on the band gap energy of TiO2", in *Environmentally Benign Photocatalysts: Applications of Titanium Oxide-based Materials*, Springer, 2010, pp. 35-111.

[42] A. Doyan, S. Susilawati, M. Taufik, S. Hakim, and L. Muliyadi, "The Optical Properties of Thin Films Tin Oxide with Triple Doping (Aluminum, Indium, and Fluorine) for Electronic Device", *Solid State Phenomena*, vol. 317, pp. 477-482, 2021.

[43] H. Chenaina, C. Messaadi, J. Jalali, and H. Ezzaouia, "Study of structural, optical and electrical properties of SnO2 doped TiO2 thin films prepared by a facile Sol-Gel route", *Inorganic Chemistry Communications*, vol. 124, p. 108401, 2021.

[44] A. Doyan, L. Muliyadi, S. Hakim, H. Munandar, and M. Taufik, "The effect of dopant material to optical properties: energy band gap Tin Oxide thin film," in *Journal of Physics: Conference Series*, vol. 1816, no. 1, IOP Publishing, 2021, p. 012114.

[45] V. Anitha, S. S. Lekshmy, and K. Joy, "Effect of Mn doping on the structural, magnetic, optical and electrical properties of ZrO2–SnO2 thin films prepared by sol–gel method", *Journal of Alloys and Compounds*, vol. 675, pp. 331-340, 2016.

[46] M. Gaidi, A. Hajjaji, R. Smirani, B. Bessais, and M. El Khakani, "Structure and photoluminescence of ultrathin films of SnO2 nanoparticles synthesized by means of pulsed laser deposition", *Journal of Applied Physics*, vol. 108, no. 6, p. 063537, 2010.

[47] S. Prayogi and M. I. Marzuki, "The Effect of addition of SnO2 doping on the electronic structure of TiO2 thin film as photo-anode in DSSC applications", *Journal of Emerging Supply Chain, Clean Energy, and Process Engineering*, vol. 1, no. 1, pp. 1-6, 2022.

[48] K. Maver, I. Arčon, M. Fanetti, S. Al Jitan, G. Palmisano, M. Valant, and U. L. Štangar, "Improved photocatalytic activity of SnO2-TiO2 nanocomposite thin films prepared by low-temperature sol-gel method", *Catalysis Today*, vol. 397, pp. 540-549, 2022.

[49] J. L. A. do Nascimento, L. Chantelle, I. M. G. dos Santos, A. L. Menezes de Oliveira, and M. C. F. Alves, "The influence of synthesis methods and experimental conditions on the photocatalytic properties of SnO2: a review", *Catalysts*, vol. 12, no. 4, p. 428, 2022.

[50] M. Selmi, F. Chaabouni, I. B. Mbarek, M. Abaab, and B. Rezig, "Effect of annealing on the optical and structural properties of TiO2 RF sputtered thin films," in *Materials Science Forum*, vol. 636, Trans Tech Publ, 2010, pp. 450-455.

[51] Y. Xu, M. Zhang, J. Lv, M. Zhang, X. Jiang, X. Song, and Z. Sun, "Preparation and characterization of heat-assisted PbS/TiO2 thin films", *Applied Surface Science*, vol. 317, pp. 1035-1040, 2014.

[52] M. K. Hossain, M. F. Pervez, M. N. H. Mia, S. Tayyaba, M. J. Uddin, R. Ahamed, M. A. S. Haque, M. Hoq, and M. A. Khan, "Annealing temperature effect on structural, morphological and optical parameters of mesoporous TiO2 film photoanode for dye-sensitized solar cell application", *Materials Science*, vol. 35, pp. 868-877, 2017.

[53] M. Basri, M. N. Asiah, M. K. bin Ahmad, M. H. Mamat, and M. Rusop Mahmood, "Electrical and structural properties of TiO2 thin film prepared at different annealing temperatures by sol-gel spin-coating method", *Advanced Materials Research*, vol. 667, pp. 371-374, 2013.

[54] M. A. Fazio, G. Vajente, A. Ananyeva, A. Markosyan, R. Bassiri, M. M. Fejer, and C. S. Menoni, "Structure and morphology of low mechanical loss TiO 2-doped Ta 2 O 5", *Optical Materials Express*, vol. 10, no. 7, pp. 1687-1703, 2020.

[55] A. Dussan, A. Bohórquez, and H. P. Quiroz, "Effect of annealing process in TiO2 thin films: Structural, morphological, and optical properties", *Applied Surface Science*, vol. 424, pp. 111-114, 2017.

[56] M. Daamouche and D. Guitoume, "Structural and Optical Properties of TiO2 Thin Films prepared by the Dip-Coating Method: Effect of Thickness and Annealing Temperature", *Advanced Materials Research*, vol. 1175, pp. 17-25, 2023.